SPATIAL ORGANIZATION OF RECEPTIVE FIELDS IN THE AUDITORY MIDBRAIN OF AWAKE MOUSE

C. V. PORTFORS,[a]* Z. M. MAYKO,[a] K. JONSON,[a] G. F. CHA,[a] AND P. D. ROBERTS,[b]

[a]*School of Biological Sciences, Washington State University, 14204 NE Salmon Creek Ave., Vancouver, WA 98686, USA*

[b]*Division of Biomedical Engineering, Oregon Health and Science University, 3181 S.W. Jackson Park Rd., Portland, OR 97239, USA*

Abstract—Efficient encoding of sensory information can be implemented by heterogeneous response properties of neurons within sensory pathways. In the auditory system, neurons in the main auditory midbrain nucleus, the inferior colliculus (IC), show heterogeneous response properties to various types of acoustic stimuli including behaviorally relevant sounds. The receptive fields of these neurons, and their spatial organization, may reveal mechanisms that underlie response heterogeneity in the IC. The mouse is becoming an increasingly popular system for auditory studies and although some studies have examined spectral characteristics in the IC, most of these have been conducted in anesthetized animals. There were two goals of this study. The first goal was to examine the frequency representation of awake mouse IC in fine spatial resolution. The second goal was to determine whether there is a spatial organization of excitatory frequency tuning curves in the IC of awake mice. We achieved these goals by histologically reconstructing locations of single and multiunit recordings throughout the IC in a mouse strain with normal hearing (CBA/CaJ). We found that the tonotopic progression is discontinuous in mouse IC, and we found that there is no clear spatial organization of frequency tuning curve types. Rather, there is heterogeneity of receptive fields in the bulk of the IC such that frequency tuning characteristics and hence the structure of excitatory and inhibitory inputs does not depend on location in the IC. This heterogeneity likely provides a mechanism for efficient encoding of auditory stimuli throughout the extent of the mouse IC. © 2011 IBRO. Published by Elsevier Ltd. All rights reserved.

Key words: inferior colliculus, mouse, tonotopy, frequency tuning, spatial organization, efficient encoding.

Sensory systems can maximize efficiency of signal processing by using as little neural activity as possible to faithfully represent natural sensory stimuli (Barlow, 2001). One strategy that cortical neurons utilize for maximizing efficient encoding is heterogeneity of receptive fields (Olshausen and Field, 1996; Lewicki, 2002). This heterogeneity can increase selectivity to specific features of a complex sensory stream and support accurate discrimination of specific sensory patterns (Chelaru and Dragoi, 2008).

Evidence of heterogeneous neural response properties has been documented in various cortical structures (Hubel and Wiesel, 1962; Ringach et al., 2002; Haupt et al., 2004), and we recently showed that heterogeneous encoding of behaviorally relevant vocalizations in the auditory midbrain of mouse is important for optimal information throughput (Holmstrom et al., 2010). In particular, information transfer in the inferior colliculus (IC) was higher than that predicted for lower brainstem nuclei, suggesting that efficient encoding strategies for complex sounds emerge in the auditory midbrain rather than the auditory cortex (Holmstrom et al., 2010).

It is not surprising that the IC displays heterogeneity in its response properties. The IC is the major processing center in the auditory midbrain (Irvine, 1992) ,as it receives massive ascending projections from all auditory brainstem nuclei (Adams, 1979; Brunso-Bechtold et al., 1981; Frisina et al., 1998) and descending projections from the auditory thalamus and cortex (Saldaña et al., 1996; Winer et al., 1998). Ascending inputs give rise to a topographic representation of sound frequency (tonotopy) in the IC that is first created in the cochlea (Merzenich and Reid, 1974; Malmierca et al., 2008). The tonotopic organization in the IC progresses from low to high frequency and has been described both as a continuous progression of frequencies (Clopton and Winfield, 1973; Merzenich and Reid, 1974) and as a stepwise progression of frequencies (Schreiner and Langner, 1998; Malmierca et al., 2008). The step-wise progression of frequencies has been related to the organization of fibrodendritic laminae within the central nucleus of the IC (Malmierca et al., 2008). Each lamina is comprised of flat, disk-shaped neurons with dendrite fields that run the length of the lamina (Oliver, 1984; Malmierca et al., 2008). Within a lamina, neurons respond to the same frequencies (i.e. isofrequency lamina) (Merzenich and Reid, 1974; Schreiner and Langner, 1998; Malmierca et al., 2008). However, the inputs to one lamina do not necessarily come from the same brainstem nuclei (Oliver, 1987), and they can be glutamatergic, GABAergic, or glycinergic (Willard and Ryugo, 1983; Saint Marie and Baker, 1990; Saint Marie, 1996; Cant, 2005; Schofield, 2005). Consequently, within an isofrequency lamina (and across isofrequency laminae), neural response properties can be diverse (Merzenich and Reid, 1974; Langner and Schreiner, 1988).

One way to determine the role of inputs in creating heterogeneity of neural response properties is to examine the excitatory and inhibitory inputs to individual neu-

---

*Corresponding author. Tel: 360-546-9434; fax: 360-546-9064.
E-mail address: portfors@vancouver.wsu.edu (C. V. Portfors).
Abbreviations: CF, characteristic frequency; IC, inferior colliculus; MT, minimal threshold; SPL, sound pressure level; USVs, ultrasonic vocalizations.

rons in different regions of the IC. One way of examining the excitatory and inhibitory inputs to individual neurons in the auditory system is to characterize frequency tuning curves (Egorova et al., 2001; Ehret et al., 2003). Previous work in the mouse IC by Ehret and colleagues (Egorova et al., 2001; Ehret et al., 2003) used the shape of frequency tuning curves to determine the structure of excitation and inhibition in different classes of neurons. Class I neurons have tuning curves similar to auditory nerve fibers and are thought to reflect direct excitatory input from the cochlear nucleus (Ehret et al., 2003). They have shallow slopes on their low frequency side and steep slopes on their high frequency side. Class II neurons have strong inhibitory sidebands resulting in narrow excitatory bandwidth and steep slopes on both the low and high frequency sides. Class III neurons are broadly tuned with little inhibition, and class IV neurons have multiple excitatory regions often with surrounding inhibitory regions.

Although the shapes of frequency tuning curves have been well documented in anesthetized mouse IC (Egorova et al., 2001; Ehret et al., 2003; Egorova and Ehret, 2008; Hage and Ehret, 2003), the organization of different types of tuning curves, and thus the organization of potentially different inputs, is less clear. There is some evidence in anesthetized mouse that class II neurons are located in the center of an isofrequency band indicating strong inhibitory inputs in this region, and neurons with less inhibition are found more peripherally (Hage and Ehret, 2003). However, there is no anatomical evidence to support this differentiation of inhibitory inputs (Loftus et al., 2010). Moreover, an in depth, three-dimensional reconstruction of frequency tuning curves throughout the extent of the IC has not yet been done in the awake mouse. Because anesthetics can influence response properties in the auditory system (Joris, 1998; Anderson and Young, 2004; Populin, 2005), it is important to understand spectral characteristics in an awake animal.

There were two goals of this study. The first goal was to examine whether the tonotopic organization of IC in awake mouse follows a discontinuous progression of frequency as has recently been documented in anesthetized rat (Malmierca et al., 2008). The second goal was to determine whether there is a spatial organization of frequency tuning curves in the IC of awake mice. We achieved these goals by histologically reconstructing locations of single and multiunit recordings throughout the IC. We found that the tonotopic progression is discontinuous in mouse IC, and we found that there is no clear spatial organization of frequency tuning curve types throughout the awake mouse IC. Rather, there is heterogeneity of receptive fields in the bulk of the IC such that frequency tuning characteristics and hence the structure of excitatory and inhibitory inputs does not depend on location in the IC. This heterogeneity likely provides a mechanism for efficient encoding of auditory stimuli throughout the extent of the mouse IC.

EXPERIMENTAL PROCEDURES

Animals

Female CBA/CaJ mice (aged 2–11 months) were used in this study; 21 mice were used to obtain single unit recordings to examine spatial organization of frequency tuning curves, and 11 were used to obtain multiunit recordings, at high resolution depth intervals, to examine features of tonotopy in awake mouse IC. The CBA/CaJ strain exhibits normal hearing sensitivity well into its second year of life (Willott, 1986, 1991, 2005), and we found no differences in neural response properties across the age range used here. Animals were housed with same gender littermates until the surgical procedure was performed. The mice were kept under a reversed 12 h light/dark schedule so that the experiments were performed during their awake period. Food and water were provided *ad libitum*. All animal care and experimental procedures were in accordance with the guidelines of the National Institutes of Health, and were approved by the Washington State University Institutional Animal Care and Use Committee.

Surgical procedures

The mouse was anesthetized with isoflurane inhalation and placed in a rodent stereotaxic frame with a mouse adapter. The head was stabilized and leveled using ear bars, taking care not to damage the eardrums. An incision was made in the scalp along the midline, and the skin reflected laterally. Using stereotaxic coordinates slightly modified from (Paxinos and Franklin, 2001) (from bregma, 3.6–5.5 mm; from midline, 0–2.2 mm), the location of the IC underneath the skull was marked with India Ink to guide the subsequent craniotomy. A hollow, metal rod (headpin) was cemented onto the skull using ultraviolet-cured dental cement. A tungsten ground electrode was then cemented into the right cerebral cortex. A local anesthetic (lidocaine) and topical antibiotic (neosporin) were applied to the wound. The animal was returned to its home cage to recover from surgery for at least 1 day prior to starting electrophysiological recordings.

On the first day of electrophysiological recordings, the mouse was given a mild sedative (acepromazine, 5 mg/kg, i.p.) so it could be restrained in a Styrofoam "sandwich" molded to the animal's body. The Styrofoam was suspended from a custom-designed stereotax, and the headpin bolted to a bar on the stereotax. The stereotax was located in a sound-attenuating chamber on an air table. A craniotomy was performed within the India Ink markings (usually 0.5 mm by 0.5 mm) to expose part of the left IC. To avoid dehydration of the brain, petroleum jelly was placed on the brain during and after electrode penetrations.

Extracellular recording procedure

Responses of single units and multiunit clusters were obtained in this study. To obtain well-isolated single unit responses and enable us to reconstruct the locations of these responses in the IC, we used micropipettes filled with 10% dextran-conjugated rhodamine (fluro-ruby) in 1 M NaCl (resistances of 20–30 MΩ). To obtain and reconstruct locations of multiunit responses, we used the same micropipettes, but broke the tip of the electrode to decrease the resistance to 5–10 MΩ. These electrodes reliably recorded multiunit clusters of 3–5 units.

Electrodes were advanced into the IC by a hydraulic micropositioner (David Kopf Instruments, Tujunga, CA, USA) located outside the acoustic chamber. Extracellular action potentials were amplified (Dagan Corporation, Minneapolis, MN, USA), filtered (bandpass, 500–6000 Hz; Krohn–Hite, Brockton, MA, USA) and sent through a spike enhancer (Fredrick Haer, Bowdoin, ME, USA) before being digitized (Microstar Laboratories, Bellevue, WA, USA; 10,000 samples/s). Neural waveforms were displayed and archived using custom-written C++ software. The software displayed raster plots, peri-stimulus time histograms (PSTHs),

and statistics on-line. Spike discrimination, spike enhancement, and time-window analysis parameters could be altered offline to analyze stored raw waveforms. Neural data were further analyzed and displayed using custom written Matlab (The MathWorks, Inc., Natick, MA, USA) programs. Each recording session lasted 4–5 h, and one to three sessions were conducted on each animal. If an animal struggled or showed discomfort during experiments, it was removed for the day and recordings were resumed on a subsequent day.

Acoustic stimulation

Pure tone stimuli were synthesized using custom-written C++ computer algorithms. Tones were 100 ms duration, had 1 ms rise/fall times and were presented at a rate of 4/s. Stimuli were output through a high speed, 16-bit digital-to-analog converter (Microstar Laboratories, Bellevue, WA, USA; 400,000 samples/s), fed to a programmable attenuator (Tucker Davis Technologies, Alachua, FL, USA; PA5), a power amplifier (Parasound), and to a leaf tweeter speaker (Emit) located 10 cm away from the mouse. The acoustic properties of the system were regularly tested using a ¼ inch calibrated microphone (Bruel and Kjaer, Denmark; model 4135) placed in the position normally occupied by the animal's ear. There was a smooth, gradual decrease in sound pressure from 6 kHz to 100 kHz of about 2.7 dB per 10 kHz. Distortion components in tonal stimuli were buried in the noise floor, at least 50 dB below the signal level, as measured by custom-designed software performing a fast Fourier transform (FFT) of the digitized microphone signal.

Stimulus protocol

Characteristic frequency (CF), threshold and excitatory frequency tuning curves were obtained from each single unit recording. Pure tones (100 ms duration) were used as search stimuli. Once a single unit was encountered and isolated, CF and minimal threshold (MT) were determined audiovisually and later confirmed with quantitative frequency tuning tests. The CF was defined as the frequency at which a unit spiked to at least 50% of the stimulus presentations at MT, and MT is the minimum threshold required to evoke a response to 50% of the stimuli at the CF.

To obtain excitatory frequency tuning curves, we presented pure tones (100 ms duration, 1 ms rise/fall time, 4/s, 200 ms recording window) across the majority of the mouse hearing range (6–100 kHz in 2 kHz steps) in 10–20 dB intensity steps from 10 dB above threshold to approximately 80–90 dB sound pressure level (SPL). Each frequency-intensity pair was presented 10–20 times. Twenty repetitions without a stimulus were used to calculate spontaneous rate.

To further examine the fine structure of tonotopy in the awake CBA/CaJ mouse IC, we recorded multiunit responses in some electrode penetrations. The protocol was the same as with the single unit recordings except that data were obtained at set intervals during each electrode penetration. After the first high quality recording was obtained in a dorsal–ventral penetration (3–5 unit cluster with high signal–noise ratio), data were then collected at 100 μm intervals. This resolution allowed us to systematically map frequency response properties throughout the extent of an electrode penetration and confirm that any results from the single unit data were not due to recording bias and missing responses in any particular region of IC. Although we measured excitatory frequency tuning curves of multiunit responses, we did not use these in the analysis of spatial organization. Similar to Malmierca et al. (2008), we used CF of multiunits to examine tonotopic organization and frequency resolution.

Histological reconstruction of recording sites

To accurately determine the three-dimensional location of each neural recording site (single and multiunit recordings) in IC, at the end of the electrode penetration we deposited the dextran-conjugated rhodamine contained in the micropipette. The iontophoretic deposits were made using positive current (+10 μA to destroy the tip of the electrode followed by +4 μA in pulsed mode [7 s on/7 s off] for 8 min). Two deposits were made to reconstruct each electrode tract. After the deposits had been made, the mouse was deeply anesthetized with sodium pentobarbital (60 mg/kg, i.p.), and once nociceptive reflexes were eliminated, the chest cavity was opened and the animal perfused through the heart with buffered 10% formalin or 4% paraformaldehyde. The brain was dissected and blocked in a plane consistent with the mouse atlas (Paxinos and Franklin, 2001). The brain was refrigerated overnight in a 30% sucrose phosphate buffer solution for cryoprotection before sectioning. Each brain was sectioned in the coronal plane using a freezing microtome at 40–50 μm thickness. Sections were collected into cold 0.1 M phosphate buffer and mounted onto microscope slides from 0.05 M phosphate buffer. Alternate sections were collected for visualization of the dextran rhodamine deposit (cleared and cover slipped with DPX) or to delineate subdivisions of the IC based on Nissl substance (stained with Cresyl Violet Acetate and cover slipped with Permount).

Data analysis

Neural response properties. Spike counts and raw waveforms were stored in the computer during data collection. In single unit experiments, raw waveforms were examined offline to ensure only spikes from well isolated single units were used in the data analysis. In multiunit experiments, raw waveforms were examined to ensure signal to noise ratios were high enough for reliable spike detection. Data were exported from the data collection software and analyzed using programs written in Matlab (The MathWorks, Inc., Natick, MA, USA). Frequency tuning curves were generated from the pure tone tests using statistical comparisons between evoked responses and spontaneous activity (Holmstrom et al., 2007).

We categorized the excitatory frequency tuning curves of single units using the classification scheme of Egorova and colleagues derived for anesthetized mouse IC (Egorova et al., 2001). Neurons were classified into class I, II, III, or IV based on the slopes of the high and low frequency sides of the excitatory tuning curve and complex response areas.

Mapping three-dimensional location of neural responses. The three-dimensional location of each single- and multiunit response was obtained by reconstructing the electrode penetrations. For each electrode penetration, the brain section(s) containing the two tracer deposits were found and digitally recorded using a Leica DF300 camera. Images were then transferred into Photoshop where the electrode penetration was reconstructed (and drawn on the section) based on the depth of the deposit sites, the dorsal surface of the brain, and the known angle of the penetration. Locations of recording sites were placed onto the reconstructed electrode tract to visualize dorsal–ventral positions. The location of each recording site in the medial–lateral plane was obtained by measuring from the midline to each recording site on the dorsal–ventral electrode penetration. The location of each recording site in the caudal–rostral plane was calculated by finding the sections containing the start and end of the IC and calculating the percent distance from caudal for each recording site. Thus, each recording site (single and multiunit recordings) was given a coordinate value in each of the three planes; dorsal–ventral, medial–lateral, and caudal–rostral.

To normalize locations of recording sites across multiple animals, the coordinates were normalized to a percentage by calculating the location as a fraction of the widest distance across the IC in the dorsal–ventral, medial–lateral, and caudal–rostral dimensions. The normalized location of each recording site was placed in a three-dimensional plot for visualization purposes and then
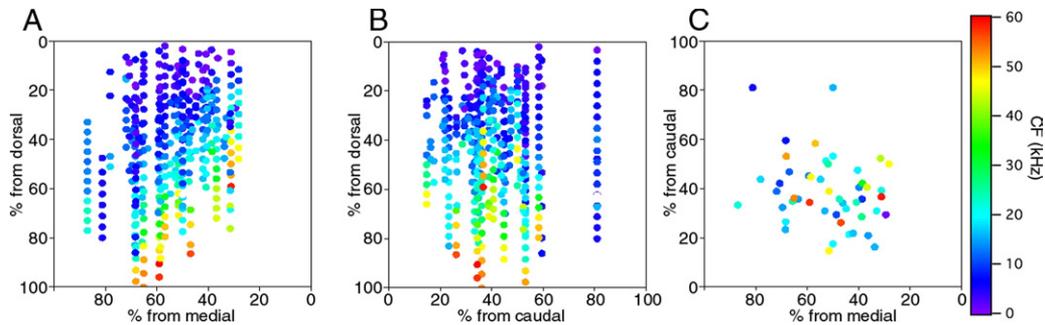
Fig. 1. Characteristic frequencies of 386 single and multiunits in the CBA/CaJ mouse IC. (A) Projection of the characteristic frequency of all single and multiunits onto the coronal plane. (B) Projection onto the sagittal plane. (C) Projection onto the horizontal plane. For interpretation of the references to color in this figure legend, the reader is referred to the Web version of this article.

placed onto a series of sections through a CBA/CaJ mouse IC stained with Cytochrome Oxidase.

To determine whether any spatial organization of frequency tuning curves exists in the IC of awake CBA/CaJ mouse, we plotted the location of each of the four tuning curve classes obtained from single unit recordings in the three-dimensions of IC as density plots. Density plots of the spatial organization of tuning curves classes were constructed by dimensional reduction. The density plots are two-dimensional histograms of the number of neurons in bins that were 10% of the total size of the IC on each side. These density plots of tuning-curve classes allowed us to quantify the spatial distribution of each class. Differences in location throughout the IC in each direction were made by comparing the distribution along each axis (medial–lateral, rostral–caudal, dorsal–ventral) with a two-tailed Student's t-test.

RESULTS

In this study we reconstructed the location of 386 neural recording sites (158 single unit and 228 multiunit) in the IC to examine the fine structure of tonotopy in the mouse and specifically determine whether tonotopy in the awake mouse IC is discontinuous as is seen in the anesthetized rat IC (Malmierca et al., 2008). Each recording site was localized in three dimensions (caudal–rostral, medial–lateral, dorsal–ventral) by histologically reconstructing each electrode penetration. The location of each recording site was then normalized and plotted in a three-dimensional plot for viewing and statistical purposes. In addition, we examined the spatial organization of types of frequency tuning curves (single units only) throughout the awake mouse IC. The goal was to determine whether there is a spatial organization of pure tone receptive fields that can suggest potential mechanisms underlying the creation of heterogeneous response properties in IC. Because receptive fields obtained by stimulation with pure tones can provide information about excitatory and inhibitory inputs to single neurons, we used the organization of these receptive fields to determine if there is any apparent organization of inputs that leads to heterogeneity in the IC.

Frequency organization in mouse IC: frequencies used in social vocalizations are under-represented

Fig. 1 shows three views of the three-dimensional scatter plot containing all the locations and CFs of the single and multiunit responses. Fig. 1A shows that CFs increased

from dorsal-to-ventral and high frequencies are only represented in a very small medial–ventral region. Fig. 1B shows that the fullest range of CFs occurs in the middle caudal–rostral portion of IC and the most rostral and the most caudal regions contain only representation of low frequencies. Fig. 1C shows the highest CF within each electrode penetration. From all three of these scatter plots, it is apparent that there is a tonotopic organization along the dorsal–ventral axis and there are proportionally few recordings with CF >40 kHz. Indeed, several of the electrode penetrations did not have any recordings of CFs in the high-frequency range where many of the behaviorally relevant social vocalizations have most of their energy (Holy and Guo, 2005; Portfors, 2007; Wang et al., 2008). It is also apparent that the IC in mouse contains a disproportionately large low frequency region with CF <20 kHz. Not surprisingly, this frequency organization is similar to that observed in anesthetized mouse IC (Stiebler and Ehret, 1985).

To ensure that our recording sites were sampled from the entire volume of the IC of awake mouse, we took the three-dimensional plot and sliced it in the caudal–rostral plane in 5% increments. We then placed all neural recording locations onto appropriate sections of real CBA/CaJ mouse IC coronal sections stained with Cytochrome Oxidase. Fig. 2 shows the organization of CFs in a series of eight sections starting caudally and progressing rostrally. From these reconstructions, it is apparent that high frequencies are represented in the most ventral–medial region of the central nucleus of IC and often are outside the central nucleus in what Stiebler and Ehret (1985) refer to as the medial zone. In addition, only low frequencies were found in the most rostral regions of the IC.

Discontinuous tonotopic organization in the mouse IC

In order to reveal any fine structure in the CF distribution and determine whether the tonotopic organization is discontinuous as has been shown in anesthetized rat (Malmierca et al., 2008), we counted the number of neurons with the same CF in 2-kHz bins. The resulting histogram shown in Fig. 3A does not have a smooth rise and fall-off but has peaks at intervals where the frequency responses are
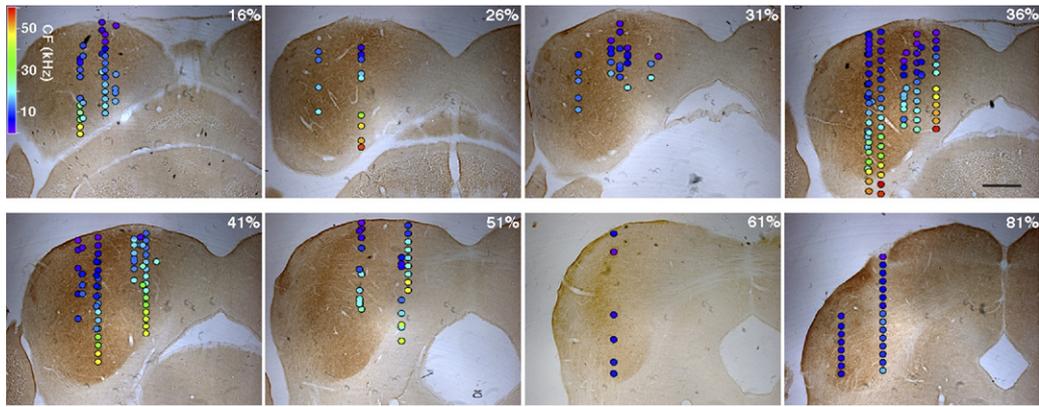
Fig. 2. Characteristic frequency of all single and multiunits superimposed onto coronal sections of CBA/CaJ mouse stained with Cytochrome Oxidase. The color represents the characteristic frequency, and the percentage of each section from the most caudal section of IC is marked in the upper right corner of each slide. Scale bar = 500 microns. For interpretation of the references to color in this figure legend, the reader is referred to the Web version of this article.

concentrated. These peaks in the frequency distribution may represent isofrequency bands as seen in the rat IC (Malmierca et al., 2008). Putative frequency bands have been marked in Fig. 3A in different colors identifying seven

isofrequency folia. The peaks are more apparent in the multiunit data because the samples were taken at regular intervals in the dorsal–ventral axis. The seven putative isofrequency folia have been overlaid on a caudal-rostral
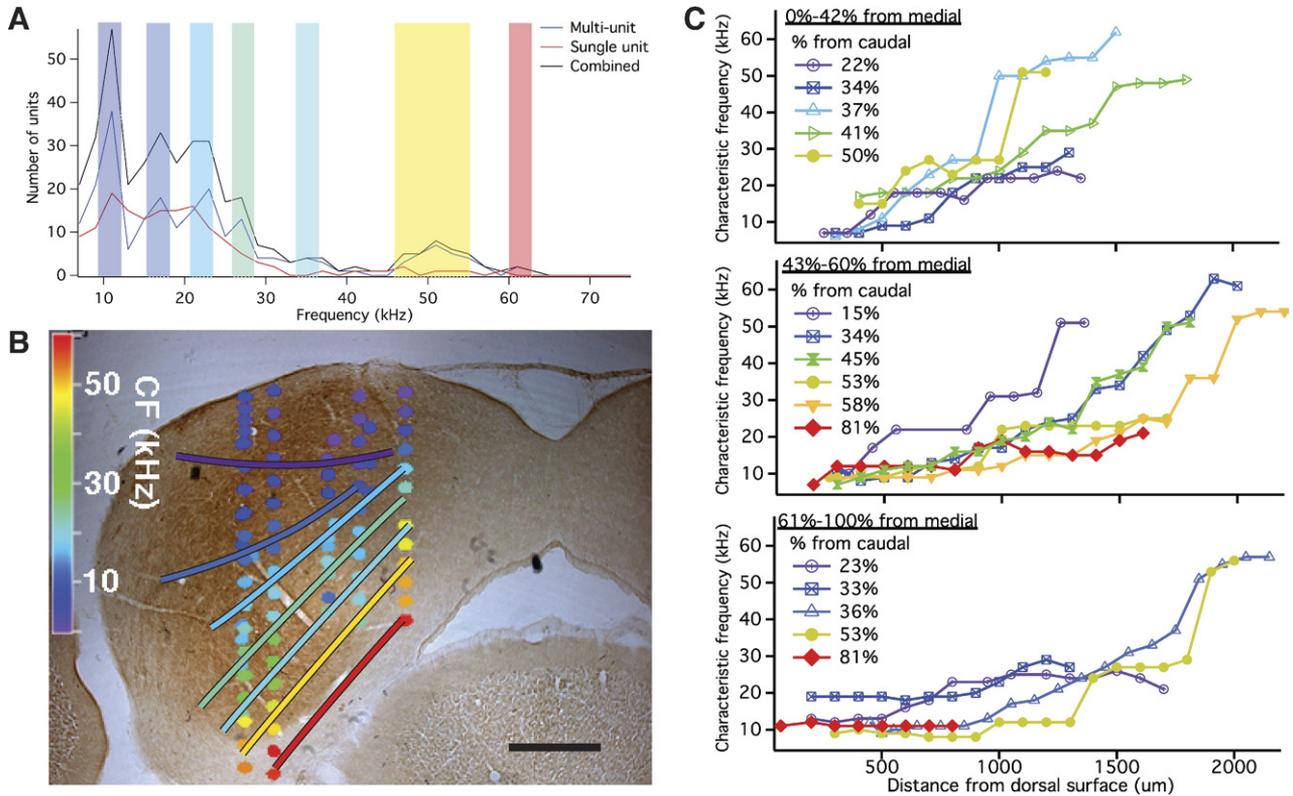

Fig. 3. Discrete isofrequency laminae are found in the mouse IC. (A) Histogram of the characteristic frequency of all units (black trace), and separate histograms for single unit (red trace) and multiunit (blue trace) recordings. The peaks suggest isofrequency lamina and are consistent between single unit and multiunit recordings. Gray bands represent putative frequency ranges of isofrequency lamina. (B) Cytochrome oxidase-stained coronal section (36% from caudal) of CBA/CaJ mouse IC with superimposed color representing nearby recorded characteristic frequencies and putative isofrequency lamina. The color of the lamina corresponds to the center of the bands. Scale bar = 500 microns. (C) Characteristic frequencies of multiunit penetrations with markers for cell locations in distance from the surface. Top graph shows penetrations close to medial, center graph shows penetrations in the middle of IC, and bottom graph shows penetrations in the lateral part of IC. The progression of characteristic frequencies from the surface does not follow a smooth increase, as suggested by tonotopy, but is broken into plateaus and jumps. For interpretation of the references to color in this figure legend, the reader is referred to the Web version of this article.

slice in Fig. 3B, revealing that the folia are not parallel in the low frequencies. In Fig. 3C we display the sequence of frequencies for the multiunit recordings, which shows a stair-step structure with plateaus as the recorded CF remains constant for up to 1000 μm of recording depth in the dorsal–ventral axis. In addition, the change in CF as a function of recording depth is not constant but appears to have sudden accelerations, or jumps in CF, in the range of 25–45 kHz.

While the frequency representation of mouse IC follows the expected tonotopy found in mammals (Merzenich and Reid, 1974; Semple and Aitkin, 1979; Schreiner and Langner, 1998; Stiebler and Ehret, 1985), previous single unit recordings in the ventral portion of awake CBA/CaJ mouse suggest there is also a nontonotopic input to this region (Portfors and Felix, 2005; Felix and Portfors, 2007). Many neurons in the ventral region have multiple excitatory tuning curves and have been classified as Class IV based on Egorova and colleagues (Egorova et al., 2001). These class IV units have characteristic frequency tuning curves in which the CF is at a high frequency (40–60 kHz), and a secondary excitatory region is located at a lower frequency; typically 10–20 kHz (Portfors and Felix, 2005). To characterize the fine resolution of how the frequency representation changes from single excitatory tuning to multiple excitatory tuning as electrode penetrations progress from dorsal to ventral, we recorded multiunit responses at 100 μm intervals.

Fig. 4 shows multiunit tuning curve shapes when arranged in sequence of penetration depth. Although recordings were done every 100 microns, we only show four recording sites in this figure for clarity of viewing. In extreme dorsal locations, the tuning curves were narrow with low CFs. As the recordings progressed more ventrally, the CF increased and the tuning curves became more diverse (both narrow and broad). At the more ventral locations, a separation developed between the CF portion of the tuning curve and the low-frequency tail, and the responses became multiply tuned. In localizing the multiunit responses histologically, we found that the mean location of all multiply tuned responses was significantly more ventral than the mean location of single excitatory tuning curves that were either narrow or broad ($P<0.01$). The mean location of all multiply tuned responses occurred at 59.0% ($\pm$22.7%) from dorsal-to-ventral. In contrast, the mean location of broadly tuned responses and sharply tuned responses occurred at 44.8% ($\pm$16.4%) and 36.9% ($\pm$16.5%) from dorsal-to-ventral, respectively. The finding that most responses in the ventral region are multiply tuned is similar to findings obtained with single unit recordings made previously in our laboratory (Portfors and Felix, 2005).

Spatial organization of frequency tuning curve shapes: heterogeneity of tuning curves throughout IC

Excitatory frequency tuning curves of 104 single units were classified according to Egorova et al. (2001) into four classes to quantify the shapes of the tuning curves. Fig. 5A
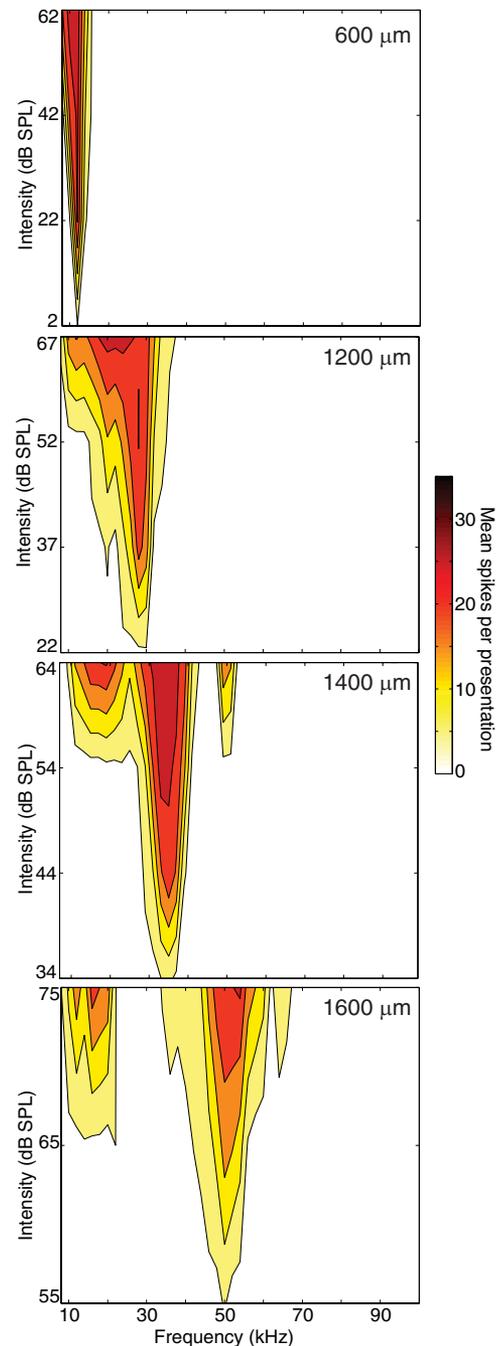

Fig. 4. Example of frequency tuning curves from a single penetration for multiunit recordings. Depth of penetration from the surface is denoted in the upper right corner of each frame. The progression from low-frequency, singly tuned units to high-frequency, multiply tuned units was typical of recordings. As recordings progress from dorsal to ventral, the tuning curve widens and then breaks into multiple response regions if the characteristic frequency becomes high enough. Multiunit recordings were obtained every 100 microns but only four recording sites are shown here for visual clarity. For interpretation of the references to color in this figure legend, the reader is referred to the Web version of this article.

shows example frequency tuning curves in each of the classes, and Fig. 5B shows the percentage of neurons in
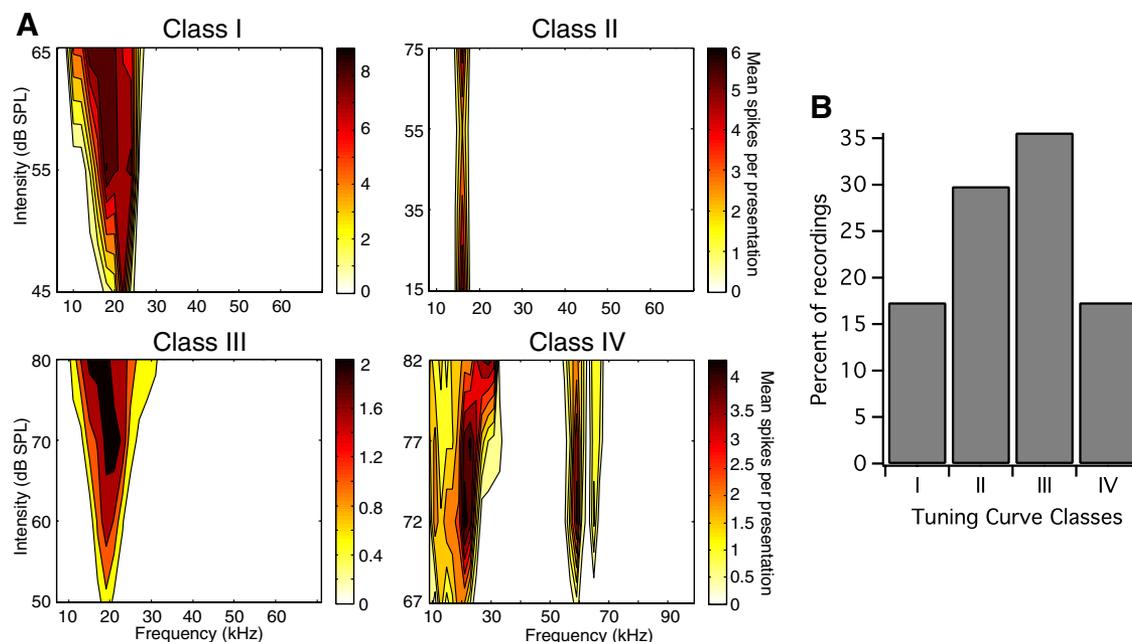
Fig. 5. Frequency tuning curve classes defined by Egorova et al. (2001), as represented by our singleunit recordings. (A) Single unit examples of the four tuning curve classes. Color scale denotes mean number of spikes for varying frequency and intensity. (B) Histogram showing the percentage of single units belonging to each frequency tuning class. For interpretation of the references to color in this figure legend, the reader is referred to the Web version of this article.

each tuning class. Class I neurons had shallow slopes on their low frequency side and steep slopes on their high frequency side. Neurons in this class had tuning curves similar to auditory nerve fibers, and 17% of the neurons recorded here were class I. Class II neurons had steep slopes on both the low and high frequency sides. Some class II neurons also had closed or tilted tuning curves because of strong inhibitory input at particular intensities, and 30% of the neurons in our sample were classified as class II. Class III neurons had broad tuning with shallow slopes on both the low and high frequency sides, and 36% of the neurons in our sample were class III. Class IV neurons had multiple excitatory regions often with complete separation between the two regions of excitation, and 17% of neurons in our sample were class IV.

To examine if there is an organization of frequency tuning curve classes in the IC of awake mouse, we plotted the density of single units in each class in each plane of the IC (Fig. 6). Density plots were obtained by binning the cells of each type in 10% increments in each plane. The two-dimensional histograms for all single units are shown in Fig. 6A for the three planes. The mean location is marked for each tuning curve class (I–IV) along with the mean for the entire population (all). The standard deviation for each class is marked in the figure with error bars. Below the two-dimensional histograms are histograms of tuning curve classes along each axis (Fig. 6B). These histograms reveal more details for the distributions of tuning curve classes.

The only separation of the tuning curve classes was found in the dorsal–ventral axis. The mean of class II neurons was significantly more dorsal than the means of

the other classes ($P<0.05$). Class II neurons were found in the dorsal 10–20% of IC, whereas almost no class I, III, or IV neurons were located there. The occurrence of class II neurons rose steadily within the dorsal 30% of IC and then declined. Single unit recordings were concentrated within the top 70% of IC, and within this dorsal–ventral range frequency tuning curve classes were heterogeneous. Except for the dorsal 10% of IC, the location of a neuron was not a good predictor of frequency tuning curve class.

As can be seen in Fig. 6A, B, there was no difference in distribution of tuning classes caudal–rostral or medial–lateral. Single units were recorded in the caudal 60% of the IC, and within this extent there was no spatial organization of frequency tuning curve classes. Single units were recorded within the 20–80% medial–lateral range of IC and again, there was no organization of tuning curve class. The distribution of the four classes was not significantly different in either the caudal–rostral ($P>0.05$) or medial–lateral dimensions ($P>0.05$).

DISCUSSION

In this study, we reconstructed the three-dimensional location of single and multiunit responses in the IC of awake CBA/CaJ mouse. We report here three main findings. First, frequencies used in social vocalizations are under-represented in the mouse IC; second, there is a discontinuous tonotopic organization in the mouse IC; and third, there is no apparent spatial organization of receptive fields within mouse IC. This final result illustrates that heterogeneity of spectral properties occurs throughout the IC of awake mouse. As heterogeneity of response properties in a pop-
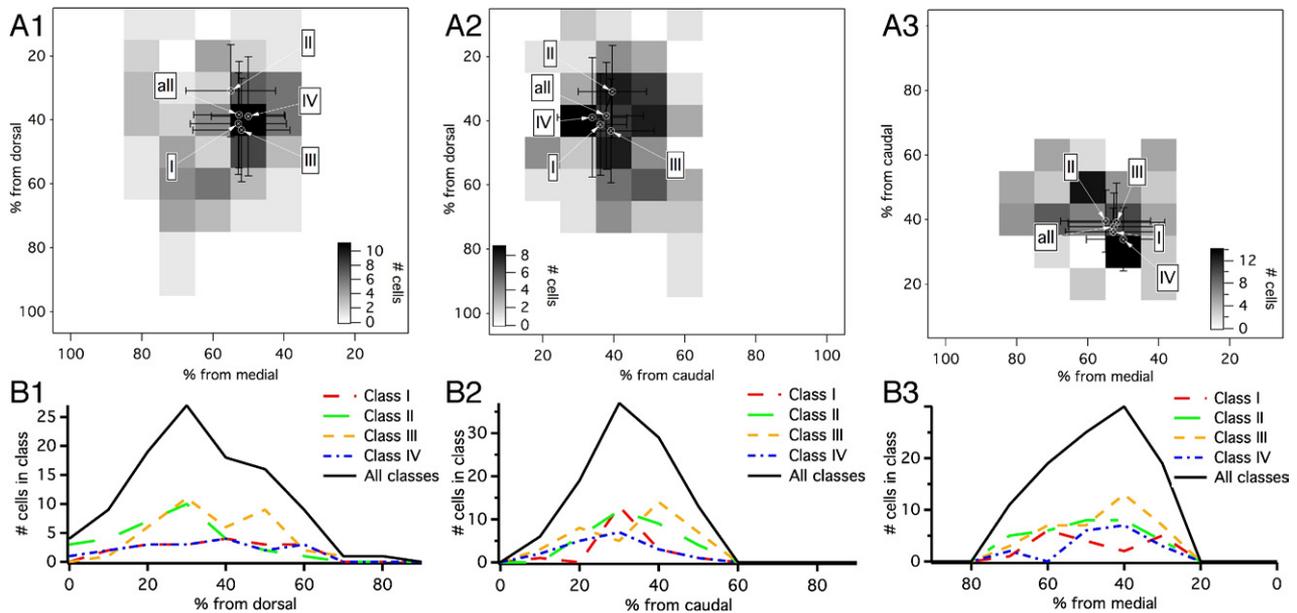
Fig. 6. Spatial distribution of frequency tuning classes in the IC. (A) Two-dimensional histograms of all single units with identifiable tuning classes separated into three planes (A1, coronal; A2, sagittal; A3, horizontal). Overlaid on each is the mean location of all the single units in each class, and error bars denote 1 standard deviation. (B) Histogram of each class along each axis (B1, dorsal-ventral; B2, caudal-rostral; B3, medial-lateral). Colors denote class type. For interpretation of the references to color in this figure legend, the reader is referred to the Web version of this article.

ulation of neurons leads to efficient encoding of sensory information (Olshausen and Field, 1996; Lewicki, 2002), our results suggest that the IC is an important structure in the ascending auditory system for efficient encoding of acoustic stimuli.

Frequencies used by mice in communication are under-represented in the mouse IC

The tonotopic organization of the awake, normal-hearing mouse IC follows the typical mammalian scheme in that low frequencies are represented dorsal–laterally and high frequencies are represented ventral–medially (Merzenich and Reid, 1974; Semple and Aitkin, 1979; Schreiner and Langner, 1998; Stiebler and Ehret, 1985). The frequency representation however, does not match the spectral content of many signals that are behaviorally relevant to mice. Both male and female mice emit ultrasonic vocalizations (USVs) with spectral content between 45 and 100 kHz during social interactions (D'Amato and Moles, 2001; Holy and Guo, 2005; Portfors, 2007). Our mapping of 386 neural responses shows that there is very little representation of frequencies greater than 60 kHz in mouse IC. There is a small peak of neurons with CFs around 50 kHz that corresponds to an area of sensitivity in the mouse behavioral audiogram (Ehret, 1983), but frequencies above 45 kHz occupy a small percentage of the total volume of the IC (this study and Stiebler and Ehret, 1985). In contrast, CFs between 15 and 26 kHz are over-represented in mouse IC (this study, Stiebler and Ehret, 1985).

The frequency organization in mouse IC suggests that few neurons will respond to mouse USVs. However, we recently showed that many neurons with low frequency tuning curves do respond to USVs (Portfors et al., 2009;

Holmstrom et al., 2010). These low frequency neurons seem to respond to USVs because combinations of ultrasonic frequencies contained in USVs generate distortion products in the cochlea that stimulate the low frequency neurons (Portfors et al., 2009). This mechanism provides the mouse with the ability to encode behaviorally relevant USVs within a large volume of IC, presumably resulting in better discrimination ability than if these signals were only encoded by the small volume of IC devoted to frequencies contained in USVs.

Discrete isofrequency lamina in the mouse IC

Similar to anesthetized rat IC (Malmierca et al., 2008), CFs do not smoothly change along the dorsal–ventral axis in mouse IC. Instead, there are discrete CF plateaus punctuated by jumps. Our results suggest a structure of seven isofrequency folia in mouse IC. In addition, the change in CF along the dorsal–ventral axis is not constant across all regions of IC. Medially, where the IC is thinner, CFs change rapidly whereas more laterally, where IC is thicker, CFs changed much more slowly and are dominated by low frequencies. These different rates of CF progression in different regions of IC are not due to the logarithmic tonotopy projected from the cochlea. Rather, there is a linear progression in the medial region and quite constant CFs more laterally. Only in the middle of IC does the progression of CF resemble a logarithmic tonotopy projected from the cochlea (Müller et al., 2005).

Heterogeneity of frequency tuning curve shapes throughout IC

One mechanism for creating heterogeneity in neural responses to sensory stimuli is to have diversity in the struc-

ture of excitatory and inhibitory inputs to different neurons. In the auditory system, frequency tuning curves can provide information about excitatory and inhibitory inputs. Previous work in the mouse IC by Egorova and colleagues (Egorova et al., 2001) used the shape of frequency tuning curves to determine the structure of excitation and inhibition in different classes of neurons. We utilized their well-documented tuning curve classification scheme to examine the spatial organization of excitatory and inhibitory inputs to IC neurons in the awake mouse.

The distribution of neuron classes found here was similar to previous studies from awake CBA mouse from our laboratory (Portfors and Felix, 2005; Portfors et al., 2009), but different from distributions obtained in anesthetized mice (Egorova et al., 2001; Ehret et al., 2003). We consistently find a higher proportion of class IV units. One reason for the discrepancy may be that the experimental paradigms are different. We present pure tone stimuli using a linear frequency scale across a wide range of the mouse hearing range (6–100 kHz) regardless of CF, whereas other studies focus the stimuli within 1–3 octaves of CF. It may be that our typical class IV neuron with a CF in the 50–60 kHz range and a secondary excitatory peak in the 15–20 kHz range would be missed with other experimental paradigms. Changes in neural responses between awake and anesthetized preparations may also explain the differences. Anesthetics are known to affect response properties in the auditory system (Populin, 2005), including receptive field characteristics (Joris, 1998; Anderson and Young, 2004). In mouse IC, anesthetics may depress neural activity in an unequal manner, such that some excitatory inputs are more suppressed (or inhibition enhanced) than others. Thus, in anesthetized animals, only the excitation corresponding to CF may be evoked.

Anesthetics may also be the cause of differences in spatial organization of frequency tuning curves found in our study and a previous study conducted in anesthetized mice (Ehret et al., 2003). Ehret and colleagues (2003) suggested that, at least within a single isofrequency band, class II neurons (sharp tuning) are located more centrally, and neurons with broader frequency tuning (classes I and III) occur more peripherally. This organization was found in both the medial–lateral and rostral–caudal dimensions. In contrast, we found that class II neurons were just as likely to occur peripherally as centrally except for a slight tendency for class II neurons to also occur in most dorsal regions compared to other neuron classes. It is also likely that histologically reconstructing the location of neural recording sites allows for greater accuracy in localizing responses and interpreting responses collected across multiple animals.

Overall, we found that there was no distinct organization of frequency tuning curves in the IC of awake CBA/CaJ mice. This lack of organization suggests diversity in excitatory and inhibitory inputs throughout most of the IC. Our data also indicate that the location of a neuron in IC cannot be used to predict the shape of its frequency tuning curve or its excitatory and inhibitory inputs. Anatomical studies support this heterogeneity of inputs to most regions

of IC. The IC receives the most diverse inputs of any auditory structure. It receives ascending input from the cochlear nucleus (Oliver, 1984, 1987), the olivary complex (Glendenning et al., 1992), and from the nuclei of the lateral lemniscus (Saint Marie et al., 1997). In addition, it receives descending input from cortical areas (Winer et al., 1998) and has rich commissural (Aitkin and Phillips, 1984) and intrinsic connections (Oliver et al., 1991). While there is evidence for specific brainstem nuclei synapsing in particular regions of IC to subdivide the IC into synaptic domains or functional zones (Aitkin and Schuck, 1985; Shneiderman and Henkel, 1987; Cant and Benson, 2006; Loftus et al., 2010), there is also evidence of heterogeneous and unpredictable patterns of input from brainstem nuclei to middle regions of IC (Loftus et al., 2010). Thus, it is apparent that neurons close together may still have unpredictable response profiles.

The means by which individual neurons in IC obtain their frequency tuning characteristics are diverse. An individual neuron may receive direct excitatory inputs from a single brainstem nucleus such that its excitatory tuning properties reflect those of auditory nerve fibers, it may receive convergent excitatory input from multiple brainstem nuclei and/or cortical structures, or it may receive both excitatory and inhibitory input from a variety of sources. Class I neurons have response properties similar to auditory nerve fibers suggesting that this class of IC neuron receives direct input from the cochlear nucleus (Ramachandran et al., 1999; Davis et al., 1999). Class I neurons are found throughout the IC suggesting that the cochlear nucleus, and in particular multipolar and stellate cells in the ventral cochlear nucleus, project over the whole IC (Kudo and Nakamura, 1988). Class III neurons have broad tuning with little evidence of inhibition and may reflect input from the ipsilateral medial superior olive (MSO) (Reetz and Ehret, 1999) or convergence of excitatory input from multiple brainstem nuclei. Because the ipsilateral MSO projects to the lateral IC, neurons in this region tend to be broadly tuned and also binaural responsive (Reetz and Ehret, 1999). However, because the mouse is high-frequency hearing animal, class III neurons may reflect input from the dorsal cochlear nucleus rather than the MSO (Spirou et al., 1993).

While class I and III neurons may inherit their response properties from different subdivisions of the cochlear nucleus, class II and IV neurons may receive convergent input from many brainstem nuclei, including those with inhibitory projections. Inhibitory input to shape class II units may come from the nuclei of the lateral lemniscus (Saint Marie and Baker, 1990), the superior olivary nuclei (Saint Marie et al., 1989; González-Hernández et al., 1996), and/or the superior paraolivary nucleus (Kulesza and Berrebi, 2000). Again, our results suggest that inhibitory projections occur across the whole of IC because class II neurons are found throughout the extent of the IC. However, it is also likely that GABAergic interneurons create some of the class II response properties in IC (Merchán et al., 2005).

Although the single unit recordings suggest little spatial structure for frequency response types, the multiunit responses and previously recorded single unit responses in very ventral regions of IC (Portfors and Felix, 2005) suggest that multiply tuned neurons are located in the ventral 40% of the mouse IC. These multiply tuned neurons have tuning characteristics that suggest that much of the IC receives low frequency inputs (<20 kHz). The tonotopy progresses from low to high frequencies along the dorsal–ventral axis such that the multiply tuned neurons have a high frequency CF in addition to a secondary excitatory tuning curve at lower frequencies (typically between 10 and 20 kHz). These tuning characteristics suggest that neurons in the ventral IC may receive convergent excitatory input from spectrally different brainstem regions (Portfors and Felix, 2005). Thus, while there is a tonotopic organization of ascending inputs to ventral IC, there may also be a nontonotopic input from a lower frequency region (Portfors and Felix, 2005). Evidence from the mustached bat also suggests the IC receives convergent tonotopic and nontonotopic inputs from different brainstem nuclei (Wenstrup et al., 1999). This convergence of different frequency inputs may lead to the same neurons in ventral IC multitasking and encoding different types of information (Portfors and Felix, 2005).

The findings from this study demonstrate that the IC is a heterogeneous structure and lacks organization of receptive fields. The potential wide diversity of inputs to the IC results in the creation of heterogeneous receptive fields and likely results in efficient encoding of acoustic stimuli, including complex sounds.

REFERENCES

Adams JC (1979) Ascending projections to the inferior colliculus. J Comp Neurol 183:519–538.

Aitkin L, Schuck D (1985) Low frequency neurons in the lateral central nucleus of the cat inferior colliculus receive their input predominantly from the medial superior olive. Hear Res 17:87–93.

Aitkin LM, Phillips SC (1984) The interconnections of the inferior colliculi through their commissure. J Comp Neurol 228:210–216.

Anderson MJ, Young ED (2004) Isoflurane/N2O anesthesia suppresses narrowband but not wideband inhibition in dorsal cochlear nucleus. Hear Res 188:29–41.

Barlow H (2001) Redundancy reduction revisited. Netw: Comput Neural Syst 12:241–253.

Brunso-Bechtold JK, Thompson GC, Masterton RB (1981) Hrp study of the organization of auditory afferents ascending to central nucleus of inferior colliculus in cat. J Comp Neurol 197:705–722.

Cant N (2005) Projections from the cochlear nuclear complex to the inferior colliculus. In: The inferior colliculus (Winer J, Schreiner C, eds), pp 115–131. New York, NY: Springer.

Cant NB, Benson CG (2006) Organization of the inferior colliculus of the gerbil (Meriones unguiculatus): differences in distribution of projections from the cochlear nuclei and the superior olivary complex. J Comp Neurol 495:511–528.

Chelaru MI, Dragoi V (2008) Efficient coding in heterogeneous neuronal populations. Proc Natl Acad Sci U S A 105:16344–16349.

Clopton BM, Winfield JA (1973) Tonotopic organization in the inferior colliculus of the rat. Brain Res 56:355–358.

D'Amato FR, Moles A (2001) Ultrasonic vocalizations as an index of social memory in female mice. Behav Neurosci 115:834–840.

Davis KA, Ramachandran R, May BJ (1999) Single-unit responses in the inferior colliculus of decerebrate cats. II. Sensitivity to interaural level differences. J Neurophysiol 82:164–175.

Egorova M, Ehret G (2008) Tonotopy and inhibition in the midbrain inferior colliculus shape spectral resolution of sounds in neural critical bands. Eur J Neurosci 28:675–692.

Egorova M, Ehret G, Vartanian I, Esser KH (2001) Frequency response areas of neurons in the mouse inferior colliculus. I. Threshold and tuning characteristics. Exp Brain Res 140:145–161.

Ehret G (1983) Psychoacoustics. In: The auditory psychobiology of the mouse (Willott J, ed), pp 13–56. Springfield, IL: Charles C Thomas.

Ehret G, Egorova M, Hage SR, Müller BA (2003) Spatial map of frequency tuning-curve shapes in the mouse inferior colliculus. Neuroreport 14:1365–1369.

Felix RA II, Portfors CV (2007) Excitatory, inhibitory and facilitatory frequency response areas in the inferior colliculus of hearing impaired mice. Hear Res 228:212–229.

Frisina D, Walton JP, Lynch-Armour MA, Klotz D (1998) Inputs to a physiologically characterized region of the inferior colliculus of the young adult CBA mouse. Hear Res 115:61–81.

Glendenning KK, Baker BN, Hutson KA, Masterton RB (1992) Acoustic chiasm v: inhibition and excitation in the ipsilateral and contralateral projections of LSO. J Comp Neurol 319:100–122.

González-Hernández T, Mantolán-Sarmiento B, González-González B, Pérez-González H (1996) Sources of GABAergic input to the inferior colliculus of the rat. J Comp Neurol 372:309–326.

Hage SR, Ehret G (2003) Mapping responses to frequency sweeps and tones in the inferior colliculus of house mice. Eur J Neurosci 18:2301–2312.

Haupt SS, Spengler F, Husemann R, Dinse HR (2004) Receptive field scatter, topography and map variability in different layers of the hindpaw representation of rat somatosensory cortex. Exp Brain Res 155:485–499.

Holmstrom L, Eeuwes L, Roberts P, Portfors C (2010) Efficient encoding of vocalizations in the auditory midbrain. J Neurosci 3:802–819.

Holmstrom L, Roberts PD, Portfors CV (2007) Responses to social vocalizations in the inferior colliculus of the mustached bat are influenced by secondary tuning curves. J Neurophysiol 47:461–481.

Holy TE, Guo Z (2005) Ultrasonic songs of male mice. PLoS Biol 3:e386.

Hubel DH, Wiesel TN (1962) Receptive fields, binocular interaction and functional architecture in the cat's visual cortex. J Physiol 160:106–154.

Irvine D (1992) Physiology of the auditory brainstem. In: The mammalian auditory pathway: neurophysiology (Popper AN, Fay RR, eds), pp 153–231. New York, NY: Springer Verlag.

Joris PX (1998) Response classes in the dorsal cochlear nucleus and its output tract in the chloralose-anesthetized cat. J Neurosci 18:3955–3966.

Kudo M, Nakamura Y (1988) Organization of the lateral lemniscal fibers converging onto the inferior colliculus in the cat: an anatomical review. In: Auditory pathway: structure and function (Syka J, Masterton R, eds), pp 171–183. New York, NY: Plenum Press.

Kulesza RJ, Berrebi AS (2000) Superior paraolivary nucleus of the rat is a GABAergic nucleus. JARO 1:255–269.

Langner G, Schreiner CE (1988) Periodicity coding in the inferior colliculus of the cat. I. Neuronal mechanisms. J Neurophysiol 60:1799–1822.

Lewicki MS (2002) Efficient coding of natural sounds. Nat Neurosci 5:356–363.

Loftus WC, Bishop DC, Oliver DL (2010) Differential patterns of inputs create functional zones in central nucleus of inferior colliculus. J Neurosci 30:13396–13408.

Malmierca MS, Izquierdo MA, Cristaudo S, Hernández O, Pérez-González D, Covey E, Oliver DL (2008) A discontinuous tonotopic organization in the inferior colliculus of the rat. J Neurosci 28:4767–4776.

Merchán M, Aguilar LA, Lopez-Poveda EA, Malmierca MS (2005) The inferior colliculus of the rat: quantitative immunocytochemical study of GABA and glycine. Neuroscience 136:907–925.

Merzenich MM, Reid MD (1974) Representation of the cochlea within the inferior colliculus. Brain Res 77:397–415.

Müller M, Hunerbein KV, Hoidis S, Smolders JW (2005) A physiological place-frequency map of the cochlea in the CBA/J mouse. Hear Res 202:63–73.

Oliver DL (1984) Dorsal cochlear nucleus projections to the inferior colliculus in the cat: a light and electron microscopic study. J Comp Neurol 224:155–172.

Oliver DL (1987) Projections to the inferior colliculus from the antero-ventral cochlear nucleus in the cat: possible substrates for binaural interaction. J Comp Neurol 264:24–46.

Oliver DL, Kuwada S, Yin TCT, Haberly LB, Henkel CK (1991) Dendritic and axonal morphology of hrp-injected neurons in the inferior colliculus of the cat. J Comp Neurol 303:75–100.

Olshausen B, Field D (1996) Natural image statistics and efficient coding. Netw: Comput Neural Syst 7:333–339.

Paxinos G, Franklin K (2001) The mouse brain in stereotaxic coordinates, 2nd ed. San Diego, CA: Academic Press.

Populin LC (2005) Anesthetics change the excitation/inhibition balance that governs sensory processing in the cat superior colliculus. J Neurosci 25:5903–5914.

Portfors CV (2007) Types and functions of ultrasonic vocalizations in laboratory rats and mice. J Am Assoc Lab Anim Sci 46:28–34.

Portfors CV, Felix RA II (2005) Spectral integration in the inferior colliculus of the CBA/CaJ mouse. Neuroscience 136:1159–1170.

Portfors CV, Roberts PD, Jonson K (2009) Over-representation of species-specific vocalizations in the awake mouse inferior colliculus. Neuroscience 162:486–500.

Ramachandran R, Davis KA, May BJ (1999) Single-unit responses in the inferior colliculus of decerebrate cats I. Classification based on frequency response maps. J Neurophysiol 82:152–163.

Reetz G, Ehret G (1999) Inputs from three brainstem sources to identified neurons of the mouse inferior colliculus slice. Brain Res 816:527–543.

Ringach DL, Shapley RM, Hawken MJ (2002) Orientation selectivity in macaque V1: diversity and laminar dependence. J Neurosci 22:5639–5651.

Saint Marie R, Baker R (1990) Neurotransmitter-specific uptake and retrograde transport of [3H]glycine from the inferior colliculus by ipsilateral projections of the superior olivary complex and nuclei of the lateral lemniscus. Brain Res 524:224–253.

Saint Marie RL (1996) Glutamatergic connections of the auditory midbrain: selective uptake and axonal transport of d-[3h]aspartate. J Comp Neurol 373:255–270.

Saint Marie RL, Ostapoff RM, Morest DK, Wenthold RJ (1989) Glycine-immunoreactive projection of the cat lateral superior olive: possible role in midbrain ear dominance. J Comp Neurol 279:382–396.

Saint Marie RL, Shneiderman A, Stanforth DA (1997) Patterns of γ-aminobutyric acid and glycine immunoreactivities reflect structural and functional differences of the cat lateral lemniscal nuclei. J Comp Neurol 389:264–276.

Saldaña E, Feliciano M, Merchan MA (1996) Distribution of descending projections from primary auditory neocortex to inferior colliculus mimics the topography of intracollicular projections. J Comp Neurol 371:15–40.

Schofield B (2005) Superior olivary complex and lateral lemniscal connections of the auditory midbrain. In: The inferior colliculus (Winer J, Schreiner C, eds), pp 132–154. New York, NY: Springer.

Schreiner CE, Langner G (1998) Laminar fine structure of frequency organization in auditory midbrain. Nature 388:383–386.

Semple MN, Aitkin LM (1979) Representation of sound frequency and laterality by units in central nucleus of cat inferior colliculus. J Neurophysiol 42:1626–1639.

Shneiderman A, Henkel CK (1987) Banding of lateral superior olivary nucleus afferents in the inferior colliculus: a possible substrate for sensory integration. J Comp Neurol 266:519–534.

Spirou GA, May BJ, Wright DD, Ryugo DK (1993) Frequency organization of the dorsal cochlear nucleus in cats. J Comp Neurol 329:36–52.

Stiebler I, Ehret G (1985) Inferior colliculus of the house mouse. I. A quantitative study of tonotopic organization, frequency representation, and tone-threshold distribution. J Comput Neurosci 238:65–76.

Wang H, Liang S, Burgdorf J, Wess J, Yeomans J (2008) Ultrasonic vocalizations induced by sex and amphetamine in m2, m4, m5 muscarinic and d2 dopamine receptor knockout mice. PLoS ONE 3:e1893.

Wenstrup JJ, Mittmann DH, Grose CD (1999) Inputs to combination-sensitive neurons of the inferior colliculus. J Comp Neurol 409:509–528.

Willard F, Ryugo D (1983) Anatomy of the central auditory system. In: The auditory psychobiology of the mouse (Willott J, ed), pp 201–304. Springfield, IL: Charles C. Thomas.

Willott J (2005) Hearing loss and the inferior colliculus. In: The inferior colliculus (Winer J, Schreiner C, eds), pp 585–682. New York, NY: Springer-Verlag.

Willott JF (1986) Effects of aging, hearing loss, and anatomical location on thresholds of inferior colliculus neurons in C57BL/6 and CBA mice. J Neurophysiol 56:391–408.

Willott JF (1991) Central physiological correlates of ageing and presbycusis in mice. Acta Otolaryngol 476:153–156.

Winer JA, Larue DT, Diehl JJ, Hefti BJ (1998) Auditory cortical projections to the cat inferior colliculus. J Comp Neurol 400:147–174.